

Eigenvalue distributions of correlated multichannel transfer matrices in strongly scattering systems

Rudolf Sprik*

Van der Waals–Zeeman Instituut, Universiteit van Amsterdam, Valckenierstraat 65-67, 1018 XE Amsterdam, The Netherlands

Arnaud Tourin, Julien de Rosny, and Mathias Fink

Laboratoire Ondes et Acoustique, Ecole Supérieure de Physique et de Chimie Industrielles de la Ville de Paris, 10 Rue Vauquelin, 75005 Paris Cedex, France

(Received 29 April 2008; revised manuscript received 7 May 2008; published 11 July 2008)

We experimentally study the effects of correlations in the propagation of ultrasonic waves in water from a multielement source to a multielement detector through a strongly scattering system of randomly placed vertical rods. Due to the strong scattering, the wave transport in the sample is in the diffusive regime. The correlation between the waves is induced when the distance between transducer elements is within the coherence region of the scattered sound. We measure the multichannel transfer matrix H , each element of which represents the signal strength between the m individual transmitters and n receivers. The observed eigenvalue distribution of the matrix HH^\dagger clearly shows the effect of correlations between channels and can be interpreted using random matrix theory. These results are of practical importance in many areas, e.g., for evaluating the information transfer capacity of such a complex scattering system.

DOI: [10.1103/PhysRevB.78.012202](https://doi.org/10.1103/PhysRevB.78.012202)

PACS number(s): 42.25.Dd, 89.70.-a

Multiple scattering of waves in random media has been studied extensively in condensed matter and also with classical waves in optics and acoustics.¹ One of the important results is that field (or intensity) correlations in time, frequency, or space can persist even after many scattering events. One example is the universal conductance fluctuations that were studied in detail in small disordered metal and semiconductor samples. With the use of theoretical methods borrowed from quantum field theory, long range correlations in multiple scattered light have also been predicted and found experimentally, in particular, for a single input channel (see, e.g., Ref. 2). Extension of the detailed scattering approach to multiple inputs and/or output channels and the correlations between them is in general difficult. In a scattering medium with n input and m output channels, an alternative approach is to model directly the statistical properties of the $n \times m$ transfer matrix H with the use of random matrix theory (RMT). The eigenvalue distribution of HH^\dagger is essential in, e.g., the transport properties of waves in the system, but also in the analysis of transfer of information as used in wireless communication. The eigenvalue distribution is highly dependent on correlations between the matrix entries, the topic of study here. In many applications RMT enables a systematic study of the influence of fluctuations in combination with imposed symmetries and correlations without the need for a detailed model for the system. Some of the early results in RMT were developed by Wigner³ to characterize eigenvalue distributions of a Hamiltonian in quantum mechanics.⁴ Even before the use in physics, random matrices were exploited in multivariate mathematical statistics as, e.g., developed by Wishart.⁵ General results were derived for the eigenvalue distribution in rectangular random matrices by Marčenko and Pastur⁶ in the 1960s.

Current developments in physics focus, e.g., on the eigenvalue distributions in quantum dots where the Hermitian character is disturbed by dissipative processes⁷ and exploit the similarity between the propagation of microwaves in a closed environment described by the Maxwell equations and

quantum mechanics described by the Schrödinger equation [see Ref. 8 for an overview]. In recent years RMT has become a powerful tool to analyze multichannel wave transfer in telecommunication.⁹ Analysis of the eigenvalue distributions with and without correlation between wireless channels is essential in estimating the error-free data rate that can be transmitted over a multichannel wireless system. This spurred activities in the microwave wireless community to verify both theoretically^{9,10} and experimentally^{11–13} the use of RMT.

The experiments we present here are performed with ultrasound in a well-defined strongly scattering environment that is difficult to realize in the wireless experiments performed so far. The ultrasound measurements allow verification of the random matrix approach for a range of square and rectangular array configurations. Ultrasounds are particularly well suited for recording such a transfer matrix since they allow a direct pointlike measurement of the field fluctuations in both amplitude and phase. We study the effects of correlations in multiple-channel systems experimentally by propagating ultrasonic waves from a multielement source to a multielement detector through a strongly scattering system of randomly placed vertical rods. The ultrasonic array setup is described in detail in Ref. 14. Ultrasonic pulses centered about 3.5 MHz are transmitted from a source array (see Fig. 1). The position of the source is moved by a computer controlled motor over distances that can be larger than the size of the receiving array or smaller than the spacing between its elements. The detector is a fixed 128-transducer array. A selection of signals captured with that array can be recorded and stored for further processing. The distance between transducer elements in the array is 0.4 mm and comparable to the wavelength of 0.42 mm at the center frequency in water. The distance between transmitter and detector is ≈ 16 cm. The random samples are made of parallel stainless steel rods with 0.8 mm diameter and placed at random with a specified surface density.¹⁴ The typical mean free path ℓ_{mf} for the wave propagation in the samples that were used is 1

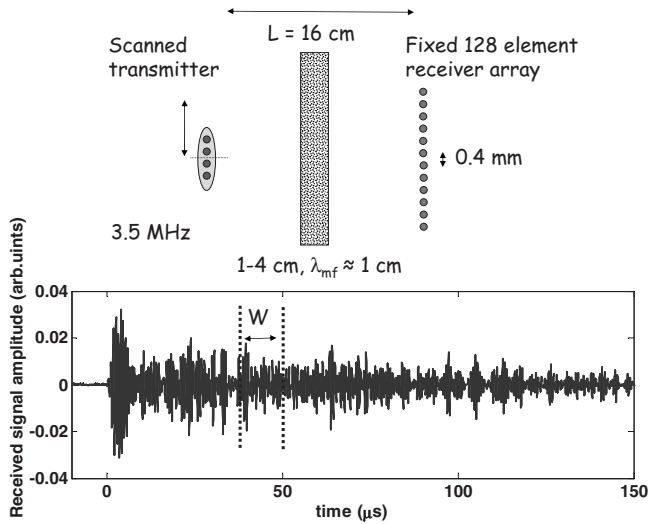


FIG. 1. The schematic diagram of the ultrasonic multichannel transmitter-receiver setup. The transmitter array is emulated by stepping the source through different positions. The receiver array uses up to 128 elements. The sample is a collection of randomly placed rods immersed in water. The signal (bottom) shows an example of a recorded signal on one of the channels for a short pulsed excitation and a 4-cm thick sample.

cm at 3.5 MHz. This is far from the Ioffe-Regel criterion $kl=1$, where corrections to diffusive behavior may be anticipated due to wave localization effects.¹

The transfer matrix is recorded by scanning the transmitter over a set of m evenly spaced locations and recording n of the responses received on the fixed array. An example of a typical signal is given in Fig. 1. A time window, W , is selected in the $n \times m$ recorded traces and used to determine the corresponding element of the transfer matrix at the central frequency by fast Fourier transform (FFT). For all results presented in this Brief Report, the window W is chosen in the tail of the traces to suppress the early part of the signal that is mainly due to the direct beam, and only the maximum of the frequency response is used. An averaging scheme has been used to enhance the statistics. Since in many of the analyzed situations m is less than the number of transducers in the array, selecting different sets of recorded transmitter-detector signals can emulate measurements for different configurations of disorder with the same source and/or detector spacing characteristics. The eigenvalues of HH^\dagger of all these sampled configurations are used in estimating the eigenvalue distribution and other statistical properties.

Figure 2 shows our experimental results for different values of $\beta=n/m$ in a situation where correlations between elements in the matrix are absent by choosing the distance between the emitting transducers much larger than the wavelength λ . In these experiments seven uncorrelated transmitters and up to 21 receivers were used. The measured values for the matrix elements of H_{mn} were close to Gaussian distributed with zero mean and finite variance. The plotted eigenvalues of HH^\dagger are scaled with the variance.

These experimental results can be understood using RMT. Marčenko and Pastur^{6,9} derived for an $m \times n$ rectangular random matrix with uncorrelated identically distributed elements that the eigenvalue distribution $f_\beta(E)$ converges rap-

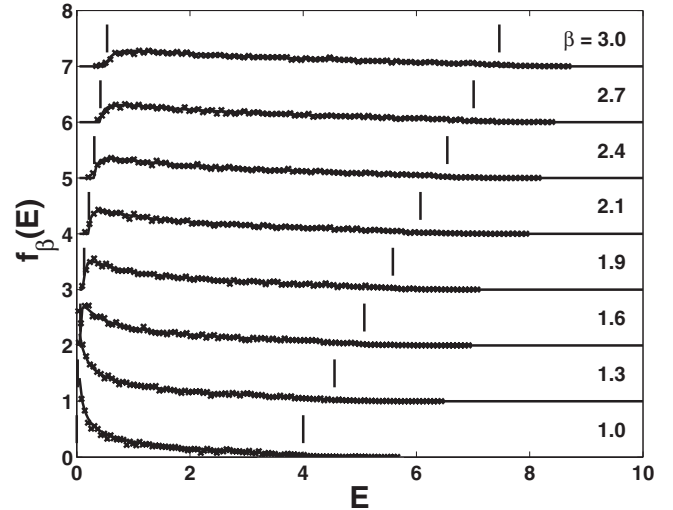


FIG. 2. Observed eigenvalue distributions (x symbols) for different values of β and scaled to the Marčenko-Pastur law Eq. (1) (line). The vertical markers indicate the interval (a,b) , where $f_\beta(E) > 0$.

idly when the size of the matrix goes to infinity with a fixed ratio $\beta=n/m$ to

$$f_\beta(E) = (1 - \beta)^+ \delta(E) + \frac{\sqrt{(E-a)^+(b-E)^+}}{2\pi E}, \quad (1)$$

with

$$a = (1 - \beta^{1/2})^2, \quad b = (1 + \beta^{1/2})^2, \quad \text{and} \quad z^+ = \max(0, z).$$

The result holds for an arbitrary distribution with zero mean and equal variance of the elements. Hence, it also holds for the Gaussian random character expected for multiple scattered waves. Due to the reciprocity principle the role of transmitters m and receivers n can be interchanged. This implicates that the results for $\beta=m/n$ also provide the results for the $\beta=n/m$ case. The convergence is rapid so that even for small values of n and m , the eigenvalue distributions are close to the Marčenko-Pastur law. This is confirmed by our experimental results in Fig. 2 that clearly show the opening of a gap near zero eigenvalues and a cutoff at larger values when $m \neq n$.

In a second series of experiments, the spacing d between elements in the transmitting array were changed from much less than λ to much larger than λ for studying the effects of spatial correlations in the scattered field. Figure 3 shows the corresponding eigenvalue distributions. The results show a clear gap near zero eigenvalues for the rectangular uncorrelated case [Fig. 3(b) and Fig. 2] that disappears when correlation is introduced. For a square configuration there is always a density near zero eigenvalue but the distribution changes when correlation is introduced. The correlation exists as soon as the spacing between elements is of the order of the coherence region in the sound field and will certainly be present when the distance becomes smaller than the wavelength. The correlation properties in random matrices have been studied theoretically, in particular, for Gaussian random elements. In the context of multivariate statistical analysis,

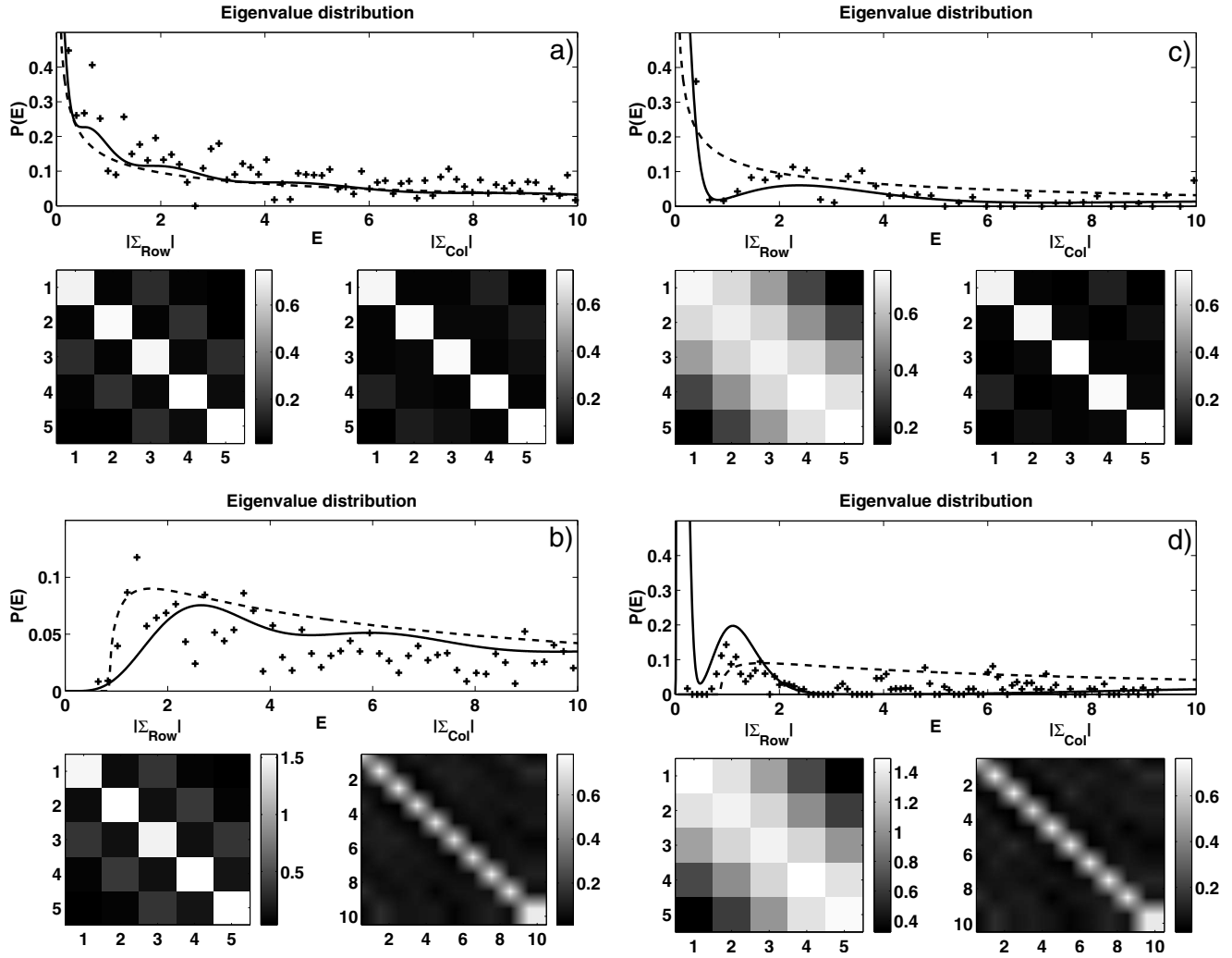


FIG. 3. The observed eigenvalue distribution and the column- and row-wise covariance matrices Σ for different array geometries and spacings between elements in the transmitter array. (a) 5×5 with large spacing, (b) 5×10 with large spacing, (c) 5×5 with spacing $< \lambda$, and (d) 5×10 with spacing $< \lambda$. The drawn curves are the distributions for a Wishart random matrix [see Eq. (3)] using the observed covariance matrix Σ_{row} . The dashed line is the Marčenko-Pastur law Eq. (1)

Wishart⁵ studied a special class of random matrices $\mathcal{W}_m(n, \Sigma) = HH^\dagger$ specified by a complex rectangular random matrix H with m rows and n columns. The random matrix H has complex Gaussian random elements with zero mean and equal variance. The correlations between elements in the transfer matrix are specified by the covariance tensor $R_{ij, i'j'} = \langle H_{ij} H_{i'j'}^* \rangle$, with the indices $i, i' = 1, \dots, m$ and $j, j' = 1, \dots, n$, and $\langle \rangle$ the average over all possible realizations of H . The row- or column-wise sum of elements of R defines an $m \times m$ or $n \times n$ covariance square matrix Σ :

$$\Sigma_{ij}^{\text{Col}} = \langle \sum_{k=1}^n H_{ik} H_{jk}^* \rangle, \quad \Sigma_{ij}^{\text{Row}} = \langle \sum_{k=1}^m H_{ki} H_{kj}^* \rangle. \quad (2)$$

If Σ is the unit matrix, correlation is absent, and the results for the Wishart matrix follow the Marčenko-Pastur law Eq. (1). The prediction of the resulting eigenvalue distribution of $\mathcal{W}_m(n, \Sigma)$ requires knowledge of the eigenvalues of the correlation matrix Σ . With the ordered eigenvalues $a_1 > a_2 > \dots > 0$ of Σ , the joint probability density function (PDF) for the eigenvalues $\lambda_1, \dots, \lambda_m$ of $\mathcal{W}_m(n, \Sigma)$ can be calculated, as well as the marginal PDF of an eigenvalue λ . The mar-

ginal PDF of a Wishart matrix $\mathcal{W}_m(n, \Sigma)$ is^{9,15}

$$q_{m,n}(\lambda) = \frac{\sum_{i=1}^m \sum_{j=1}^m \mathcal{D}(i,j) \lambda^{n-m+j-1} e^{-\lambda/a_i}}{m \det \Sigma^n \prod_{\ell=1}^m (n-\ell)! \prod_{k<\ell} \left(\frac{1}{a_\ell} - \frac{1}{a_k} \right)}, \quad (3)$$

where $\mathcal{D}(i,j)$ is the (i,j) th cofactor of the matrix described by

$$\mathbf{D}_{\ell k} = \frac{(n-m+k-1)!}{a_\ell^{-n+m-k}}.$$

The denominator in Eq. (3) shows that the distribution tends to be strongly varying for situations where the eigenvalues of Σ are almost degenerate.

The column- and row-wise covariance matrices Σ for the system are plotted in Fig. 3 for a square and a rectangular transmitter array geometry. That there is correlation between elements is obvious from the nonzero off-diagonal elements

in Figs. 3(c) and 3(d), and the correlation vanishes when the distance between the elements becomes larger [Figs. 3(c) and 3(d)]. The predicted distributions for Wishart matrices $\mathcal{W}_5(5, \Sigma)$ and $\mathcal{W}_5(10, \Sigma)$ with the covariance matrices observed in the experiment are plotted with a full line, while the uncorrelated Marčenko-Pastur result is plotted with a dashed line. In the experiment the covariance between receiver (or transmitter) elements is determined by the multiple scattered waves from the source locations. Using a covariance that mimics the spatial correlation of a fully developed speckle pattern, $\Sigma_{ij} = J_0(|(i-j)|/\Gamma)$ with the correlation length $\Gamma = 0.7$ and J_0 , the zero-order Bessel function fits the behavior for the row-wise covariance displayed in Fig. 3. In all other cases $\Gamma = 0$. With the relatively small number of 5000 configurations realized in the experiment, a good estimate of the random matrix elements and their correlations is not converged yet and is still fluctuating strongly. The associated scatter does not allow a detailed comparison of the experimentally obtained distributions and the theoretical distributions expected from Eq. (1) or Eq. (3). However, from the data we can conclude that the observed distributions follow the correlated results more closely, in particular, near the small eigenvalues.

Our results are of interest in the context of multiple input multiple output (MIMO) communication through disordered media, where the key element is the ability of the communication system to exploit independent channels of propagation.^{16,17} For example, for radio signals multiple paths arise because of scattering and multiple reverberation off the buildings or indoors; similar multipath phenomena are also frequently encountered in underwater acoustics. On a first approximation, the more heterogeneous and scattering the medium is, the more degrees of freedom there are to communicate through it, and it becomes then advantageous to use several transmitters and receivers. However, the number of independent channels can be drastically reduced if

some scattering events induce correlations and especially spatial correlations as demonstrated in field trials with wireless microwave communication.¹¹⁻¹³ Also restrictions in the form of conduits and keyholes impose correlations that influence the eigenvalue spectrum of HH^\dagger .^{18,19}

The estimate of the maximum attainable transfer rate that can be supported without any errors of transmission uses a multichannel extension of the Shannon capacity.^{20,21} At the heart of the analysis is the transfer matrix H and the distribution of eigenvalues of HH^\dagger . In the case that the channel strength is unknown to the transmitter, the “ergodic capacity” of the MIMO channel is given by $C = \sum_{i=1}^m \log_2(1 + E_s/nN_0E_i)$, with E_i the eigenvalues of HH^\dagger , E_s the total average transmitted power, and N_0 the noise power at each receiver. Using the eigenvalue distribution for a characteristic ensemble of realizations of H , an estimate of the average and the fluctuations of the transfer capacity for the available signal-to-noise ratio at the receivers can be made. As demonstrated in Fig. 3, the correlation between channels increases the probability of a low eigenvalue, and the MIMO capacity can be significantly reduced. For example, the mean of the eigenvalue distributions for the 5×10 array configuration with correlations at the transmitter site [Fig. 3(d)] is a factor ≈ 2.1 smaller than the mean for the uncorrelated case [Fig. 3(b)]. It is also interesting to point out that using more transmitters than receivers (or vice versa) can increase the capacity. At best the number of independent channels is given by $\min(n, m)$, but the probability of low eigenvalues is decreased in the case of rectangular matrices: the weighting of the signal-to-noise ratios at the receivers is more favorable.

This work is part of the research program of the “Stichting voor Fundamenteel Onderzoek der Materie (FOM),” which is financially supported by the Nederlandse Organisatie voor Wetenschappelijk Onderzoek (NWO).

*sprik@science.uva.nl; URL: <http://www.science.uva.nl/wzi>

¹P. Sheng, *Introduction to Wave Scattering, Localization, and Mesoscopic Phenomena* (Academic, New York, 1995).

²F. Scheffold, W. Härtl, G. Maret, and E. Matijevic, *Phys. Rev. B* **56**, 10942 (1997).

³E. Wigner, *Ann. Math.* **67**, 325 (1958).

⁴C. W. J. Beenakker, *Rev. Mod. Phys.* **69**, 731 (1997).

⁵J. Wishart, *Biometrika* **A20**, 32 (1928).

⁶V. A. Marčenko and L. A. Pastur, *Math. USSR. Sb.* **1**, 457 (1967).

⁷P. J. Forrester, N. C. Smith, and J. J. M. Verbaarschot, *J. Phys. A* **36**, R1 (2003), and other articles in this special issue.

⁸H.-J. Stöckmann, *Quantum Chaos: An Introduction* (Cambridge University Press, New York, 1999).

⁹A. Tulino and S. Verdú, *Found. Trends Commun. Inf. Theory* **1**, 1 (2004).

¹⁰R. R. Müller and H. Hofstetter, *IEEE Trans. Antennas Propag.* **1**, 472 (2001).

¹¹A. Taparugssanagorn, M. Alatosava, V. M. Holappa, and J. Ylitalo, *IEEE 65th Vehicular Technical Conference 2007*, pp. 481–485.

¹²H. Nishimoto, Y. Ogawa, T. Nishimura, and T. Ohgane, *IEEE Trans. Antennas Propag.* **55**, 3677 (2007).

¹³D. Chizhik, J. Ling, P. W. Wolniansky, R. A. Valenzuela, N. Costa, and K. Huber, *IEEE J. Sel. Areas Commun.* **21**, 321 (2003).

¹⁴A. Derode, V. Mamou, and A. Tourin, *Phys. Rev. E* **74**, 036606 (2006).

¹⁵S. H. Simon and A. L. Moustakas, *Phys. Rev. E* **69**, 065101(R) (2004).

¹⁶G. J. Foschini and M. J. Gans, *Wireless Pers. Commun.* **6**, 311 (1998).

¹⁷A. L. Moustakas, H. U. Baranger, L. Balents, A. M. Sengupta, and S. H. Simon, *Science* **287**, 287 (2000).

¹⁸D. Chizhik, G. Foschini, M. Gans, and R. Valenzuela, *IEEE Trans. Commun.* **1**, 361 (2002).

¹⁹R. Sprik, *Phys. Rev. E* **72**, 037602 (2005).

²⁰C. E. Shannon, *Bell Syst. Tech. J.* **27**, 379 (1948).

²¹E. Telatar, AT&T-Bell Technical Memorandum, 1995; *Eur. Trans. Telecom.* **10**, 585 (1999).